# Nanomaterials for spectroscopic and electrochemical detection of metal ions

by

**Sruti Bhaumik**

A.B. Chemistry, Bryn Mawr College, 2006

Submitted to the Graduate Faculty of the

School of Arts and Sciences

in partial fulfillment

of the requirements for the degree of

Master of Science in Chemistry

University of Pittsburgh

2009

UNIVERSITY OF PITTSBURGH

School of Arts and Sciences

This thesis was presented

by

Sruti Bhaumik

It was defended on

February 17, 2009

and approved by

Dr. David Waldeck, Professor, Chemistry

Dr. Nathaniel Rosi, Assistant Professor, Chemistry

Thesis Director: Dr. Alexander Star, Assistant Professor, Chemistry

Copyright © by Sruti Bhaumik

2009

**Nanomaterials for spectroscopic and electrochemical detection of metal ions**

Sruti Bhaumik M.S.

University of Pittsburgh, 2009

Techniques for the analysis of metal ions including ion exchange chromatography, UV-Vis-NIR spectroscopy, fluorescence spectroscopy, cyclic voltammetry, adsorptive stripping voltammetry, and use of field-effect transistors are reviewed. The advantages and disadvantages of each method are described. Development and incorporation of nanotubes as practical materials for rapid and portable sensing applications with improved selectivity and sensitivity over previous methods is discussed.

Interactions of chelating molecules ferrozine and neucuproine with $Fe^{2+}$ and $Cu^{+}$, respectively, are studied via UV-Vis-NIR spectroscopy. Interactions of these molecules with carbon nanotube networks are monitored spectroscopically and electrochemically to elucidate the charge transfer mechanism between analyte species, chelating ligands and the carbon nanotube network. Synthesis and characterization of carbon nanotube networks are discussed. This information will contribute to forming a framework of metal ion sensing using carbon nanotubes and aid in the rational design of nanoscale sensors for environmental, medical, biological and defense contexts.

## TABLE OF CONTENTS

## LIST OF TABLES

## LIST OF FIGURES

## LIST OF SCHEMES

## PREFACE

I thank my advisor Dr. Star and my colleagues in the group for all the advice and assistance with equipment and experiments. Special thanks to Albert Stewart for his help on the scanning electron microscope and x-ray diffractometer in the engineering department, Tom Harper for transmission electron microscope training, Lori Neu, Tom Gasmire, and the staff of the instrument and machine shops.

I am grateful for funding from the Department of Chemistry, the Bayer Corporation, and the National Energy Technology Laboratory of the U.S. Department of Energy.

Finally, I thank my friends and family for their constant encouragement and generous support.

# 1.0 INTRODUCTION

Identifying and quantifying metal ions in mixtures occurring in habitats and in organisms is a key method of monitoring pollution and health.[1] There have been many procedures and instruments developed to achieve this objective, all of which take advantage of the inherent differences in metal ions including mass to charge ratio, polarity, solubility, fluorescence, redox behavior and interaction with complexing agents.

Techniques such as chromatography[2], spectroscopy[3] and electrochemical analysis[4] are the most widespread for metal ion detection. Emerging technologies including nanoscale electrodes and sensors are being developed to improve resolution and detection limits in metal ion determination, as well as enabling the production of equipment that is less expensive, more portable and yielding rapid results.

The advantages and disadvantages of ion exchange chromatography, fluorescence spectroscopy, electrochemistry and use of chelating molecules as they apply to metal ion detection will be discussed. In addition, carbon nanotubes are explored as a versatile and sensitive material amenable to identification and quantification of metal ions in environmental and physiological settings.

Analysis of transition metal ions are of particular interest, as these ions have been associated with toxicity and disease. Since many enzymes require metal ions as cofactors in

order to carry out metabolic function, deficiency or excess of metal ions have consequences in the health and survival of the organism.

Water-soluble chelating ligands selective to $Fe^{2+}$ and $Cu^{+}$ are employed in conjunction with thin films of carbon nanotube networks. These metal-ligand interactions are studied by UV-Vis spectroscopy and electrical conductance of carbon nanotube networks when exposed to metal ions and metal-ligand complexes are monitored. Results of experiments on carbon nanotube-based substrates for spectroscopic and electrochemical metal ion identification and quantification are reported.

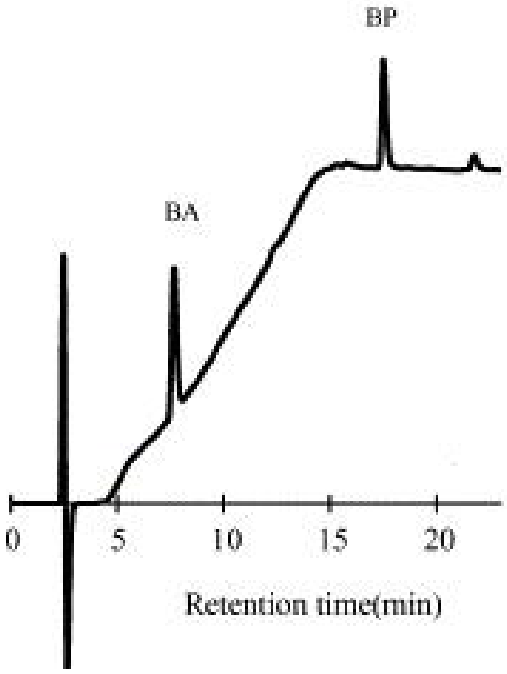


**Figure 1:** HPLC chromatogram for the separation of benzoic acid (BA) and benzoyl peroxide (BP). Adapted from Reference 6.

## 1.1 ION EXCHANGE CHROMATOGRAPHY

Metal ions dissolved in a solution (mobile phase) are flowed over a column made of insoluble material. This column is packed with beads of material which have opposite polarity to that of the ions under study. Ions are separated by affinity with the column, that is, the ions with least affinity for the column are eluted most rapidly, thus having shorter retention times, and the ions that have the strongest affinity for the column are eluted from the column last and have longer retention times. Thus a particular ion will maintain its retention time under the same conditions: column, mobile phase, pressure,

temperature; enabling the identification of this ion in a mixture. A UV-Vis absorbance detector is often present at the end of the column for analyte identification and concentration may be calculated from the absorbance using Beer's Law. Peaks produced on the chromatogram correspond to the retention times of the ions, and calculation of peak area or height gives information on ion concentration. Parameters such as column type and dimensions, flow rate, and strength of mobile phase may be further modified to optimize separation and resolution. The type and packing of column material greatly influence the efficiency of the analysis. As packing of column beads reduces the pore size, there is less exchange of the analyte with the column leading to increased linear velocity of analyte resulting in improved resolution of the chromatogram.[5,6] It is important to note that columns with tighter packing and smaller pore sizes are more costly.

Identification and quantification of metal ions is thus repeatable and rapid (time scale in range of minutes) when using this instrumentation. However, optimization of this system to analyze multicomponent samples with minimal interference can be challenging. Techniques such as gradient elution,[7,8,9,10] which employs the gradual increase of the strength (polarity or acidity) of the mobile phase to better differentiate the relative affinities of each ion for the column, result in improved separation. At high pH, all metal ions are retained at the front of the column. As the pH is reduced stepwise, metals are eluted and give sharp peaks on the chromatogram. The most tightly retained metal ions are eluted under the most acidic conditions.

Another strategy is coating the stationary phase with ligands that chelate metal ions with greater selectivity than ion exchange materials usually present in columns. For example, preconcentration and separation of $Al^{3+}$ in tap water was achieved by coating a column with Chrome Azurol S (shown at left), a ligand which complexes trivalent metal ions. However, peak

broadening occurs when the metal is retained to this column for longer than five minutes and limits the number of metal ions separated in one run, leading to reduced efficiency of this method.[11]

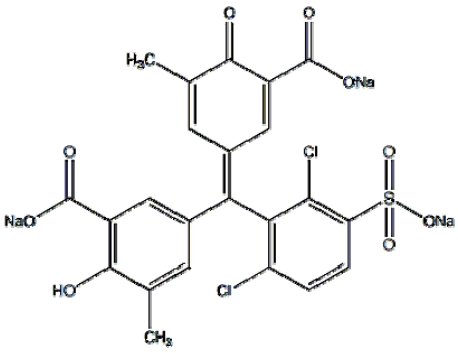


**Figure 2:** Chrome Azurol S

These drawbacks may be avoided by adding chelating ligands to the mobile phase instead. Selectivity and efficiency are improved as ligand loading is increased without adversely affecting column capacity. Metal ions are eluted in order of their increasing stability constants, stronger complexed ions are eluted faster as they are less retained on the column. An added bonus of this approach is the formation of colored metal-ligand complexes in the mobile phase that may be detected spectroscopically at the end of the column. These complexes tend to absorb in the UV-Vis range.

## 1.2 UV-VIS SPECTROSCOPY WITH CHELATING LIGANDS

Metal ions and electron rich molecules may interact according to Lewis acid-base behavior, in which the metal ions act as the Lewis acid, accepting electron density from the Lewis-basic molecule acting as a ligand. An interesting consequence of this charge-transfer complexation is the occurrence of a significant absorbance in the UV-Vis range (that does not exist when the metal or ligand are dissolved on their own), often associated with a change in the color of the solution. Absorbance and concentration are related by Beer's Law, so a calibration

curve of absorbances associated with known concentrations of metal-ligand complexes may be used to detect ions.

Selectivity for a metal ion is influenced by the nature of the complexing agent, its electronic structure (aromaticity and availability of lone pairs on atoms such as nitrogen, oxygen, and sulfur to interact with metal ions), and the size of the cavity accommodating the ionic radius of the analyte of interest. The phenanthroline structure (shown below) has been a common moiety for binding transition metal ions while crown ethers and calixarenes show preferential binding to group I and group II metals. [12]

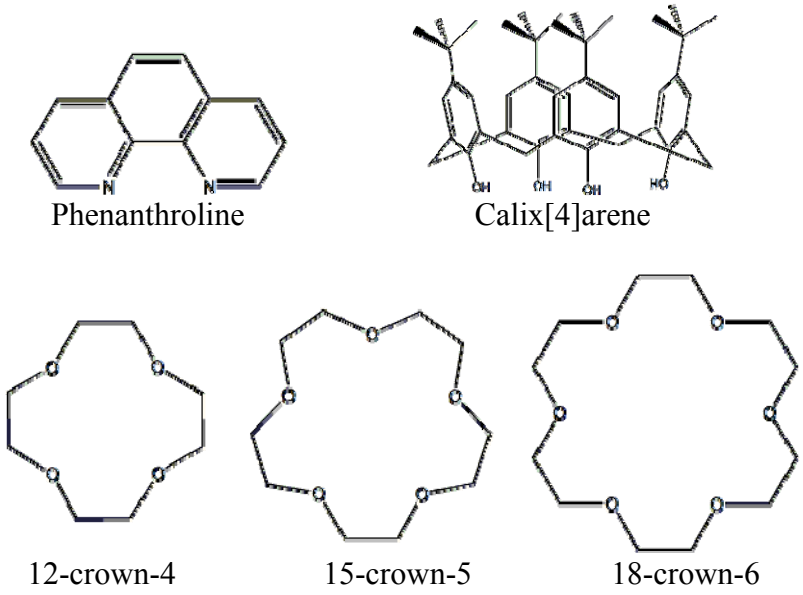


**Figure 3:** Common molecules employed for chelation of metal ions.

As with other analytical methods, the selectivity and sensitivity of this method is compromised by pH, as the conjugation of the metal-chelating ligands is disrupted by protonation and deprotonation. Thus, pH must be carefully buffered to the level at which ligand

is at its most stable conformation and yields optimal selectivity and sensitivity of the desired analyte.

Many of these ligands are commercially available and affordable. Further modification of these ligands with functional groups or adjustment of the type and number of atoms in the complexation site can change the chemistry and size of the cavity thus fine-tuning the selectivity and sensitivity of the ligand for a particular metal ion. The time to collect results is dependent on the wavelength range used and the scan rate of the instrument. Portable UV-Vis spectrometers enabling on-site analysis have recently become more prevalent. Since purification and extraction of marine or physiological samples are necessary prior to UV-Vis study, real-time analysis is challenging.

## 1.3 FLUORESCENCE SPECTROSCOPY

Detection of metal ions is primarily carried out by their quenching of fluorescence of highly conjugated molecules. Usually this analysis of metal ions is associated with their extraction from an aqueous solution into an organic medium, as the metal ion complexes with the fluorophore. Examples of this system include $Fe^{2+}$ characterized in viable cells using rhodamine B-[(1-10-phenanthrolin-5-yl)aminocarbonyl]benzyl ester)[13] and $Hg^{2+}$ detected by 5,10,15,20-tetraphenylporphyrin in a polymer electrode.[14]

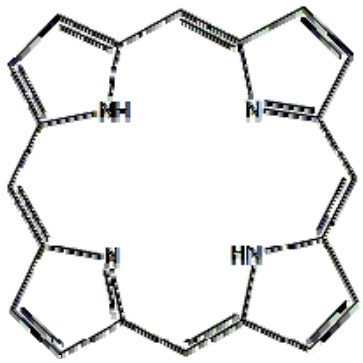

**Figure 4:** Porphyrin

Porphyrins (general structure shown at left) are often used in fluorescence spectroscopy as they produce high quantum yield and large Stokes shift (difference in excitation and emission wavelength). They are also amenable to metal ion recognition as the porphyrin moiety boasts a highly conjugated double bond system and mobile π electrons. Quenching of fluorescence occurs as metal ions provide pathways competing with emission as well as disrupting the conjugation structure of the fluorophore due to charge transfer and complexation.

The advantages of using fluorescence spectroscopy to measure ions as a function of quenching include high selectivity and sensitivity without the need for pre-concentration and digestion of samples. Levels of detection in the parts-per-billion (ppb) range have been obtained.[15,16] Sensitivity may be compromised by changes in pH of the sample solution. as the conjugated system of the fluorophore becomes modified upon protonation, fluorescence is prevented and metal ion complexation is affected by the change in the cavity of the ligand. As a

result, measurement of cation concentration by fluorescence quenching is not possible. Therefore, the sample must be carefully buffered.

Metal ions may also be studied by the degree of fluorescence amplification. This type of analysis is carried out by using a weakly fluorescent molecule and chelating it with a metal ion, yielding highly fluorescent complexes. Morin (3,5,7,2'-4' pentahydroxy flavone) exhibits enhanced fluorescence ($\lambda_{ex}$= 420 nm, $\lambda_{em}$=488 nm) when complexed to $Al^{3+}$ at pH 4.8.[17] The complexation reaction is described in Scheme 1 below. Interferences from other ions do not occur at this pH, as complexation of morin with other ions is limited to pH 7. However $Fe^{3+}$, which quenches fluorescence irreversibly at pH 4.8 due to strong complex formation, renders the morin-aluminum fluorescence sensor useless. This may be resolved by reducing all $Fe^{3+}$ ions to $Fe^{2+}$, leaving the ligand to bind only with $Al^{3+}$. Quenching may be further prevented by containing the metal-ligand complexes in micelles which prevent entry of species that may interfere with fluorescence.[18] The limit of detection of this morin-based fluorescence sensor is $1x10^{-6}$ M $Al^{3+}$ (0.027 ppm) with linear response from $10^{-4}$ M and $10^{-6}$ M.

Fluorescence analysis of metal ions can be obtained in minutes, but the instrumentation may be expensive and bulky and therefore not conducive to on-site metal ion detection.

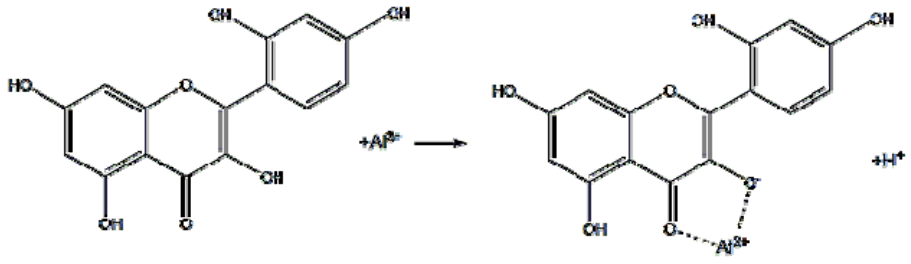


**Scheme 1:** Morin (3,5,7,2'-4' pentahydroxy flavone) forming complex with $Al^{3+}$

## 1.4 ELECTROCHEMICAL ANALYSIS

The redox properties of metal ions are useful in analysis as reduction potentials as they are repeatable and consistent for each species. Cyclic voltammetry, adsorption stripping voltammetry, and use of field-effect transistors have been employed to quantify ions selectively and rapidly with high sensitivity. However, as with any analytical method, interference effects may be present, and these methods have varying sensitivities for analytes and environments.

In the case of cyclic voltammetry (CV) the analyte is dissolved in an electrolyte to which three electrodes are inserted: working, reference and auxiliary. The analyte is studied by sweeping a voltage, set by computer software and potentiostat, across the electrolyte and the redox reaction occurs on the surface of working electrode. In one direction of the voltage sweep, the analyte is oxidized; when the voltage is reversed, the analyte is reduced. Thus, there is little loss of sample in this technique. Current generated is dependent on the reduction potential and concentration of the ion and a peak is produced when the swept voltage reaches the standard potential of oxidation or reduction of the analyte. The reference electrode is necessary for the measurement of potential; the auxiliary electrode is necessary for the measurement of current, and prevents any side reactions with the working electrode and solvent from interfering with the analysis.

The area of the peak produced upon redox reaction of desired species can be used to determine the concentration of analyte. As with other analytical methods, CV traces of a series of standards may be obtained under identical potential sweep and scan rate conditions, and this calibration is used to quantify the amount of a particular redox active species in a sample. Thus, CV in an easy and effective way to identify the abundance of ions in solution based on their

electrochemical activity and can be used to distinguish between oxidation states. CV has a notably low level of detection, in the range of $10^{-6}$ M, and analysis times ranging in minutes.

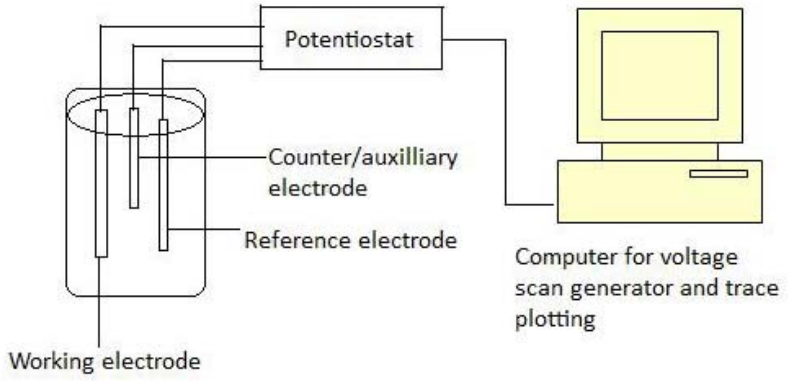


**Figure 5:** Diagram of cyclic voltammetry setup. Analyte is dissolved in electrolyte in sample vial. Electrodes are immersed in this sample solution, current is measured as voltage is swept and redox properties of analyte are obtained to identify and quantify ions.

Stripping voltammetry has a superior limit of detection, up to $10^{-10}$ M, making it useful for trace ion analysis in the sub-ppb (parts-per-billion) range.[19] A substance reacts with the electrolyte and results in the formation of a product that is adsorbed on the working electrode. The substance reacts with mercury on the working electrode to form an amalgam in the anodic[20] stripping voltammetry (ASV) method, and forms an insoluble mercury salt layer in cathodic stripping voltammetry (CSV). Then a potential scan is applied to strip this analyte from the electrode, the resulting currents are proportional to the amount of metal ion in the sample solution. In ASV, a negative potential (0 to -1.2 V versus SCE) is applied to oxidize the analytes pre-concentrated on the electrode, while on the other hand, a positive potential is applied to reduce the analyte from the electrode in CSV. The position of peak potential is particular to each metal ion, thus enabling identification of many components of a solution. Interference from other compounds may be minimized by modifying the deposition time and potential.[21] The levels of sensitivity are improved by using thin films or microelectrodes of mercury or working electrodes composed of bismuth. [22,23]

More recently, field-effect transitors (FETs) are increasingly employed in metal ion detection, as they provide rapid analysis and low levels of detection. The conductance of these transistors is driven by an applied potential and is dependent on the type of majority carrier (holes or electrons) of the current. Gate voltage applied to device and electronic environment is affected upon exposure by electron-withdrawing or electron-donating molecules to an FET device, resulting in increase or decrease of conductance as a function of concentration of the analyte molecule. FETs generally consist of semiconducting materials, and are classified as *p*-type if holes are the majority carriers, and *n*-type if electrons are the majority carrier. Therefore, conductance of *p*-type FETs would increase upon exposure to electron-withdrawing molecules, and increase for *n*-type FETs upon exposure to electron-donating molecules.[24]

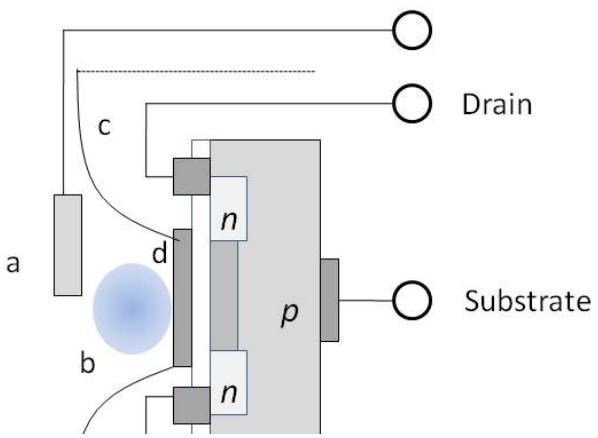


**Figure 6:** ISFET (ion-sensitive field-effect transistor) device, a) reference electrode, b) analyte solution, c) epoxy, d) gate insulator. Adapted from Reference 25.

This device (general scheme shown at left) is durable, rugged, small, inert in harsh environments, possesses low electrical impendence and yields rapid response to analyte molecules.[25] The main electronic scheme is highly reproducible and suitable for mass production while the function of the transistor may be customized by modifying the gate insulator with monolayers,[26] conductive polymers,[27,28] or carbon nanotubes[29,30,31] to improve signal to noise ratio, or endow the device with greater selectivity and sensitivity to the analyte of interest.[25]

As discussed above, many interesting techniques exist for the determination of metal ions in solutions, and each system has its

analytical limitations. The strengths and weaknesses of ion exchange chromatography, UV-Vis spectroscopy, fluorescence spectroscopy, electrochemical analysis including cyclic voltammetry, and stripping voltammetry and use of field effect transistors are summarized on the next page.

| Technique | Detection Limit | Strengths | Weaknesses |
|---|---|---|---|
| **Ion-exchange chromatography**[32] | 4.2 ppm $Co^{2+}$<br>4.6 ppm $Mn^{2+}$ | High selectivity and sensitivity which may be further improved by gradient elution and use of chelating ligands. | Separation efficiency affected by peak broadening<br>Time consuming<br>Expensive equipment |
| **UV-Vis spectroscopy**[33] | 340 ppb $Fe^{3+}$<br>120 ppb $Fe^{2+}$ | Inexpensive, rapid, selective and sensitive | pH dependent<br>Signal interference from sample matrix |
| **Fluorescence spectroscopy**[14, 17] | 6.5 ppb $Zn^{2+}$<br>3.0 ppb $Al^{3+}$ | High sensitivity and selectivity, particularly when using ligands that specifically chelate metal ions<br>Rapid analysis | pH dependent<br>Signal interference from sample matrix<br>Bulky, expensive equipment<br>Difficult to perform on-site analysis |
| **Cyclic voltammetry**[34] | 1 ppb $Cd^{2+}$<br>0.1 ppb $Cu^{2+}$ | High sensitivity and selectivity<br>Rapid analysis | pH dependent<br>High scan rates may generate resistance or noise interfering with analysis |
| **Stripping voltammetry**[22,23] | 0.3 ppb $Pb^{2+}$<br>0.8 ppb $Ni^{2+}$ | High sensitivity and selectivity<br>Simultaneous detection of multiple metal ions<br>Portable, automated, in-situ applications<br>Low cost | Stripping occurs on mercury electrode, which can be toxic, unsuitable for in-situ biological settings<br>Bismuth and carbon electrodes are being developed to address this issue |
| **Field-effect transistors**[35,36] | 1 ppm $Cu^{2+}$<br>0.1 ppm $Ca^{2+}$ | FETs easily fabricated and mass produced<br>Rapid analysis | Further functionalization necessary (nanoparticles, DNA, polymers, etc) to endow selectivity and sensitivity of FET towards metal ions |

**Table 1:** Summary of strength and weaknesses of various analytical techniques.

## 2.0 CARBON NANOTUBES IN ANALYSIS

The bonding and structure of carbon nanotubes (CNTs) are responsible for the strength, stability, flexibility and sensitivity to their electronic environment, thus making carbon nanotubes a suitable material for analytical applications. CNTs are visualized as a rolled up sheet of graphite, with each carbon bonded to its adjacent carbon via $sp^2$ hybridized orbitals and electron density delocalized over $2P_z$ orbitals perpendicular to the nanotube wall. [37]

MWCNTs (multi-walled carbon nanotubes) were reported by Iijima in 1991[38] and are characterized as bundles of concentric tubes. SWNCTs (single-walled carbon nanotubes) were reported in 1993 by Iijima[39] and Bethune[40], et al. CNTs were first produced by the arc discharge method by Iijima in 1993 and were classified as single-walled nanotubes based on their morphology in that they consisted of only one tube. Additional methods to synthesis carbon nanotubes include laser ablation and chemical vapor deposition. Methods of synthesis will not be discussed further, as the analytical applications of carbon nanotubes are the focus of this work. The behavior of nanotubes as individuals and as ensembles will be considered as they are exploited for analytical and electronic purposes. The helicity and diameter of CNTs

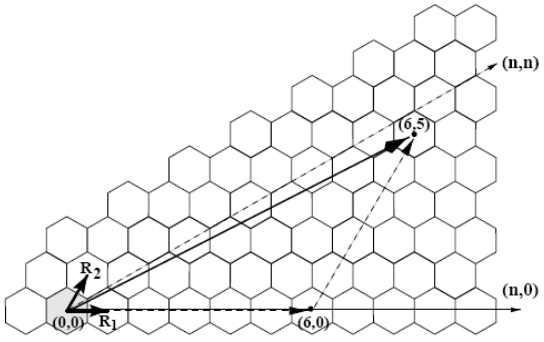


**Figure 7:** Visual representation of roll up vectors (n,m) on graphite sheet.Electronic properties influenced by roll up vectors. Adapted from Reference 41.

influence their properties. Helicity and diameter are related to the so-called roll up vectors involved in the transformation of a flat sheet of graphite into a cylindrical tube. These vectors are shown at left.[41] The electronic properties of the nanotube are an important consequence of these roll up vectors. CNTs are classified as metallic (if n-m=3k, 0 where k is any integer) or semiconducting (if n-m≠3k). These characterizations determine how these nanotubes are applied. A metallic film is preferred for transparent conducts and electrochemical applications while a semiconducting film is better suited for use in field-effect transistors (FETs) and sensing applications.[42,43,44] However,it is difficult to separate metallic and semiconducting SWNTs. A random network of as-produced SWNTs will contain ⅓ metallic nanotubes and ⅔ metallic nanotubes, and such a mixture is adequate to transport current as long as the nanotube density is above the percolation threshold. This is related to the overlap of the nanotubes and conduction along a percolating path occurs when the average length of the nanotubes is greater than their average separation.[39]

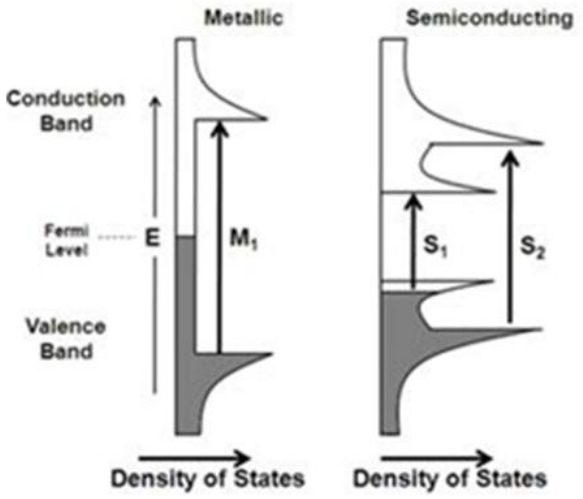


**Figure 8**: van Hove singularities of metallic and semiconducting nanotubes. Adapted from Reference 44.

The diameter and helicity of nanotubes are two determining factors of their electronic and chemical behavior. It has been shown that as the diameter increases, the band gap of the nanotube decreases. It is postulated that as the diameter is related to the degree of overlap of the electron orbitals.[45] According to solid state physics of nanotubes, the valence and conduction bands of SWNTs are confined into discrete energy bands (van Hove singularities). They are

shown in the diagram at left. The shaded regions in this diagram represent the occupied states in the valence band. According to this model, the separation between the valence and conductance band is the band gap. The ease of transport of charge, and the magnitude of transitions $M_1$, $S_1$ and $S_2$ shown above are dictated by the size of this band gap. These transitions between van Hove singularities,[46] are observed in UV-Vis-NIR spectra of carbon nanotubes.[47]

The heights and location of the UV-Vis-NIR absorbance bands of the nanotubes shift as electron density is transferred between the nanotube and analyte or dopant. For example, if the HOMO of the analyte lies above the valence band of the nanotube energetically, than electron density may be donated to the nanotube, resulting in an increase of UV-Vis-NIR absorbance of the latter. On the other hand, if the LUMO of the analyte lies below the valence band of the nanotube energetically, than electron density will be removed from the nanotube and withdrawn by the analyte, resulting in a decrease of UV-Vis-NIR of the nanotubes. Since this charge transfer behavior between nanotubes and chemical species is observable spectroscopically, it should be monitored by conductance measurements. This is the rationale behind using nanotubes in electrochemical detection applications. [48]

Theoretically, the perfect graphitic walls of the carbon nanotubes are not reactive but they may have defects such as phenol, ketone, aldehyde and carboxylic groups.[49,50,51,52] Exposure to radio-frequency gas or air plasma treatment[40,53] introduces defects and oxygen-, nitrogen-fluorine-containing functional groups to ends and walls of carbon nanotubes, affecting reactivity and resistivity, taking advantage of the versatility of this material in synthesis and analysis. Nanotubes may also be noncovalently modified with DNA[54], peptides,[55,56] nanoparticles[57] and other ligands via van der Waals forces, hydrogen bonding, and π-π stacking interactions.[58,59,60] These and other modifications can result in nanotubes that are either *p*-type (where holes as

majority carriers) or *n*-type (where electrons are majority carriers) semiconductors. Doping of CNTs enables their use as field effect transistors (FETs) for power devices and sensors for ions, gases, and biological species. Exposure of analytes to the FET modulates its conductance as a function of the identity and concentration of the analyte; this will be elaborated in a later section.

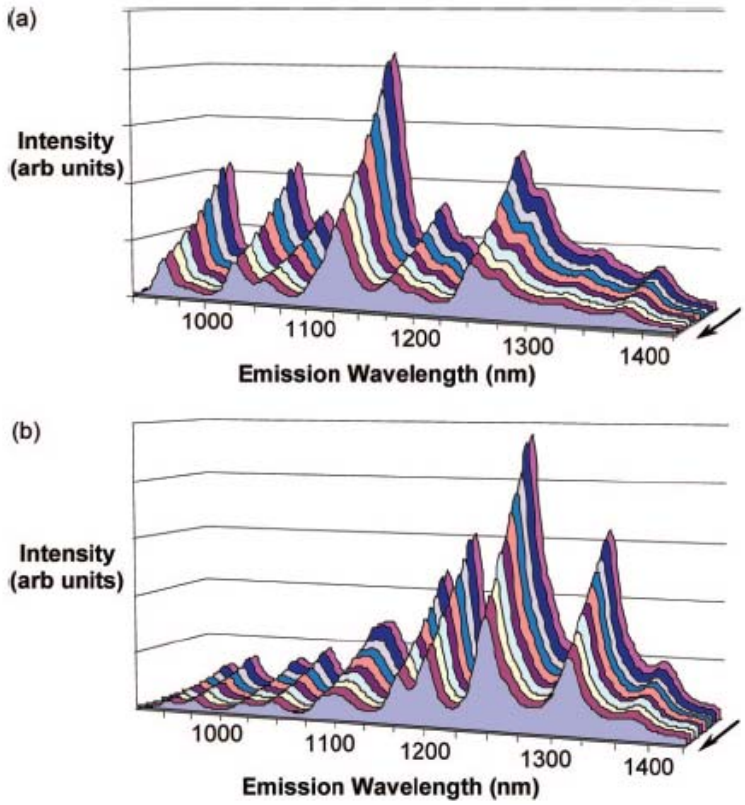


**Figure 9:** Quenching effect of $Cu(OAc)_2$ on SDBS-SWNT fluorescence intensity. Arrows signify increasing metal ion concentration. a) excitation at 660 nm b) excitation at 785 nm. Adapted from Reference 59.

## 2.1 FLUORESCENCE QUENCHING OF CARBON NANOTUBES BY ADSORBED SPECIES

Fluorescence in SWNTs is caused by the formation of an exciton when light is absorbed by the nanotube. The high surface area and propensity for quantum confinement[61] enable SWNTs to display exceptional adsorption of ions and molecules. Fluorescence of nanotubes (influenced by their diameter, which dictates their band gap) can be quenched as a result of aggregation and adsorption of species on the sidewalls of carbon nanotubes.[62] The adsorbed metal ions provide alternate non-radiative decay pathways that

compete with fluorescence resulting from excitation. The larger the ionic radius of the ion, the greater the efficiency of quenching that occurs for a SWNT, and the smaller the diameter of the SWNT, the greater the quenching effect of a particular $M^{2+}$ ion.[59]

Treatment of SWNTs with surfactants such as sodium dodecyl sulfate (SDS) and sodium dodecylbenzenesulfonate (SDBS) has been shown to improve fluorescence of SWNTs.[63,64] After SWNTs were coated with SDBS, they were exposed to 660 and 785 nm excitation radiation and fluorescence intensity was recorded. Increasing concentrations of aqueous solutions of metal ions $CuSO_4$, $Cu(OAc)_2$, $CuCl_2$, $CoSO_4$,$Co(OAc)_2$, $CoCl_2$, $NiSO_4$, $Ni(OAc)_2$, and $NiCl_2$ were added. Inductively-coupled plasma atomic emission spectroscopy (ICP-AES) was used to determination the final concentration of metal ions on the nanotubes. The pH did not vary significantly following metal ion addition. The metal ion-SDBS-SWNTs were then exposed to 660 and 785 nm excitation radiation. For all metal ions studied, all semiconducting nanotubes exhibited decreased fluorescence intensity as metal ion concentration increased. Peak shifts did not occur, only decrease in intensity, irrespective of the excitation wavelength used. The degree of quenching did depend on the metal ion. Fluorescence was recovered upon the addition of EDTA to chelate the metal ion; thus demonstrating the reversibility of the nanotube fluorescence quenching caused by metal ions.

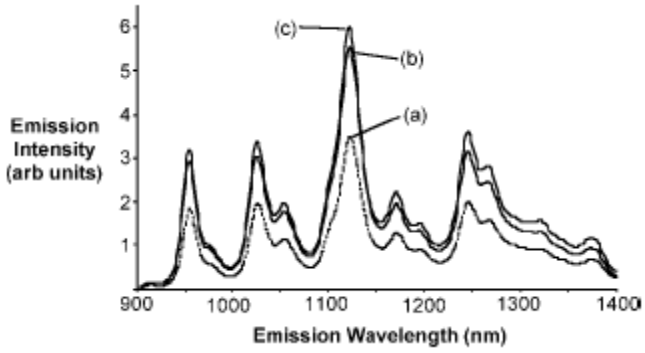


**Figure 10:** Fluorescence of SDBS-SWNTs using 660 nm excitation in the presence of $CoCl_2$ (3.0 mM) before (a) and after (b) additionof EDTA (15 mM) showing the recovery of fluorescence with the addition of EDTA. The SDBS-SWNT fluorescence spectrum in the presence of EDTA (15 mM) but in the absence of metal ion quencher is shown for comparison (c). Adapted from Reference 60.

Stern-Vollmer quenching constants were calculated for each metal ion. These quenching constants were not related to atomic number or redox potential of the metal. Quenching was not due to UV-Vis absorbance by metal ions since none of the metals absorb at the excitation wavelengths used (660 and 785 nm). However, UV-Vis absorbance was observed when the metal ion was present in combination with SDBS, suggesting that may filter the incident radiation resulting in diminished fluorescence following excitation.

When controlling for the anion ($Cl^-$, $SO_4^{2-}$, $OAc^-$), quenching efficiency followed the general trend of $Ni^{2+} < Co^{2+} < Cu^{2+}$. When controlling for the transition metal ion, quenching efficiency followed trend of $Cl^- \approx SO_4^{2-} > OAc^-$.[60] This trend was attributed to the different complexation ability of the cation with the anion and the ionic volume of the complex and its relationship to the degree of quenching. Expressed concisely, the larger the ionic volume of the complex, the greater the quenching.

By systematically monitoring the quenching of nanotube fluorescence with respect to the added ion and ionic volume of complex formed, the workers were able to form a rationale behind the quenching behavior.

Basically, the identity of the cation has agreater effect on nanotube fluorescence quenching than the anion used, independent of the nanotube diameter. Brege, *et al* offer the following explanation: the metal ion forms a complex with SDBS, which screens the incoming radiation and provides alternate pathways for the SWNT exciton formed after excitation, thus quenching fluorescence. This metal ion effect on quenching is in competition with the ionic-volume effect related to the counterion. As the quenching was demonstrated to vary according the cation added, these phenomena pave the way for the use of the modulation of carbon nanotube fluorescence intensity as a strategy for metal ion detection.

## 2.2 ELECTROCHEMICAL ANALYSIS OF METAL IONS USING CNT-CONTAINING ELECTRODES

CNTs have a porous structure, large specific surface area promoting rapid electron transfer with analytes.[65] Electrodes composed of CNTs have demonstrated stable electrochemical behavior, resistance to surface fouling or damage, and a voltammetric response characteristic of steady-state radial diffusion.[66,67] Nanoelectrodes enable miniaturization, increased mass transport rate, decreased susceptibility to solution resistance, and diminished interference resulting in improved resolution of analysis (signal-to-noise ratio).[68] Adsorptive stripping voltammetry (AdSV) has proven to be a highly sensitive method to detect trace levels of ions easily and rapidly, boasting a remarkably low limit of detection in the ppb range. The large surface area of the carbon nanotubes enables strong interfacial accumulation of adsorbents. CNT-containing working electrodes for stripping voltammetry have been used to analyze heavy metal ions such as $Cu^{2+}$, $Co^{2+}$, $Hg^{2+}$, $Pb^{2+}$ at the ppb range relevant to environmental and medical monitoring.[69,70,71]

Glassy carbon electrodes coated with MWNT thin films have been used for the pre-concentration of $Hg^{2+}$.[70] This electrode yielded enhanced stripping peak current (particularly when $Hg^{2+}$ was dissolved in HCl) and exhibited minimized interference by other ions in solution such as $I^-$.

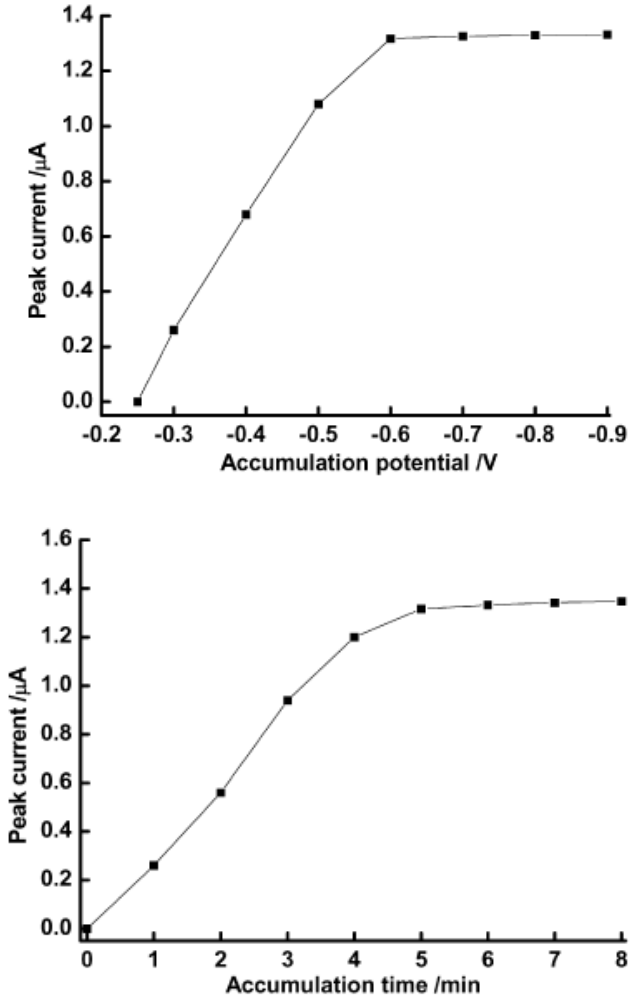


**Figure 11:** Determination of accumulation time that yields highest peak current (top) Determination of optimal accumulation potential for highest peak current (bottom). Adapted from Reference 68.

Mercury was accumulated on the MWNT-coated electrode for 5 minutes at 0.60 V, this accumulation time and voltage gave the optimal peak current. Stripping peak current was proportional to concentration for the range $8\times10^{-10}$–$5\times10^{-7}$ M $Hg^{2+}$ and the detection limit was calculated to be $2x10^{-10}$ M after 5 minute accumulation time. These results were highly reproducible and exhibited minimal interference from ions such as $Cd^{2+}$ and $Fe^{3+}$ which only gave 5% error in the measurement of trace $Cd^{2+}$ concentration.

Glassy carbon electrodes were modified with MWNTs and conducting polymer poly(1,2-diaminobenzene) (poly(1,2-DAB)) by simultaneous electrochemical deposition. These materials, due to their high surface area and capacitive storage, exhibit environmental stability and conductivity superior to that of traditional glassy carbon electrodes.

MWNTs and poly(1,2-DAB) were dissolved in potassium perchlorate and perchloric acid to which the glassy electrode was submerged and multipulse potential was applied from -0.2 V to 0.7 V. This was followed by oscillation and cyclic voltammetry at the same potential range as

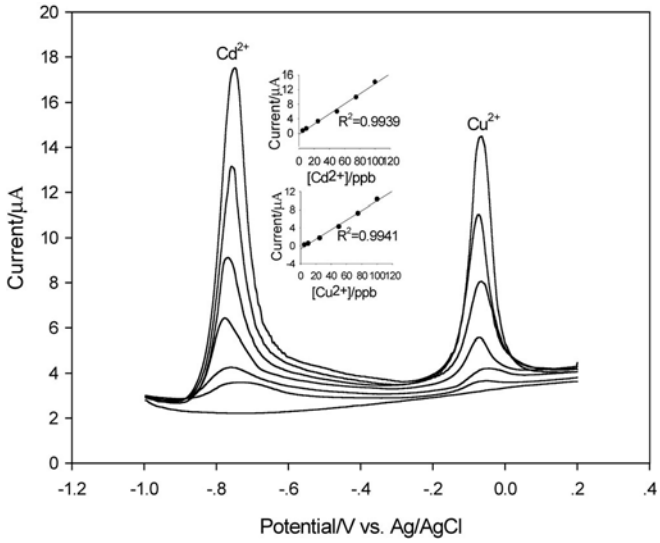


**Figure 12:** Current vs. potential for increasing concentrations of $Cd^{2+}$ and $Cu^{2+}$. Inset: Linear calibration of Current vs. concentration of $Cd^{2+}$ and $Cu^{2+}$. Adapted from Reference 63.

the previous step. The change in the morphology of the surface of these electrodes was verified by scanning electron microscopy (SEM).

The metals were deposited at -1.0 V for an accumulation time of 3 minutes. Peak currents of $Cd^{2+}$ and $Cu^{2+}$ were measured at -0.76V and -0.06 V, respectively, upon square wave stripping voltage sweep from -1.0 V to 0.2 V. The limits of detection for these ions dissolved in 0.1 M sodium acetate-acetic acid buffer solution at pH 4.4 were 0.25 ppb for $Cd^{2+}$ and 0.33 ppb for $Cu^{2+}$ thus demonstrating that MWNT-1,2-DAB-modified working electrodes boast an impressive degree of sensitivity. When analyzing a real wastewater sample, the limits of detection of each ion by this method (11.2 ppb $Cd^{2+}$ and 31.2 ppb $Cu^{2+}$) were comparable to those of atomic absorption spectroscopy (9.6 ppb $Cd^{2+}$ and 32.5 ppb $Cu^{2+}$). [63]

Carbon nanotube electrode arrays (CNT-NEAs) were employed to detect $Pb^{2+}$.[69] These arrays were grown from Ni nanoparticles deposited on a Cr-coated Si substrate. Plasma-enhanced chemical vapor deposition was carried out to grow the aligned carbon nanotube arrays. The formation of this product was verified with SEM. This vertical alignment was maintained even after application of epoxy and subsequent

spin-coating. CNTs embedded in the Cr-Si have open ends that have fast electron transfer rates suitable for electrochemical sensing.

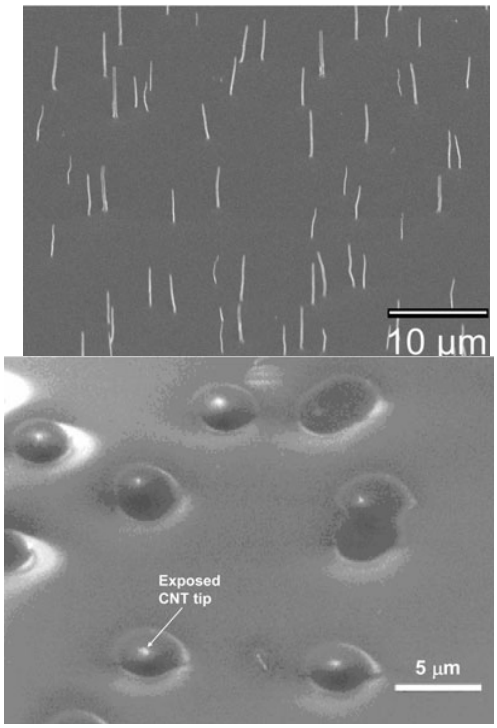


**Figure 13:** Aligned Carbon nanotube arrays on Cr/Si substrate

Cyclic voltammetry was used to evaluate the electrochemical behavior of this array. This array served as the working electrode which was immersed in a stirred solution of $K_3Fe(CN)_6$. Platinum wire and saturated calomel electrode (SCE) were used as counter and reference electrodes, respectively. Square wave voltammetry was used to study the quantitative behavior of this working electrode with an analyte solution. In this case, Ag/AgCl was used as the references electrode and solutions were degassed with $N_2$ for a few minutes prior to analysis.

Hg was deposited on the working electrodes prior to the detection of $Pb^{2+}$ by using 5 ppm $Hg^{2+}$ in 0.1 M $NaNO_3$ solution and applying -1.1 V potential for 5 minutes. Electrodes were rinsed with ultrapure water, immersed in 0.1 M $NaNO_3$ supporting electrolyte containing $Pb^{2+}$ and -1.1 V was applied in order to electrodeposit the $Pb^{2+}$ onto the Hg-coated electrode. The formation of the Hg-Pb amalgam is necessary for the detection of $Pb^{2+}$. Potential is scanned from -1.1 V to -0.1 V, and the response peak of lead appeared at -0.45 V.

As a consequence of the small electrode surface, the CNT-NEAs yielded a smaller current than regular bare glassy carbon electrodes in supporting electrolyte solution, and resulted in a smaller Ohmic drop, leading to better defined peaks in the voltammograms, giving measurements of $Pb^{2+}$ concentration with greater linearity with current. The detection limit of Pb2+ was 1 ppb after a 3 minute preconcentation period.[69]

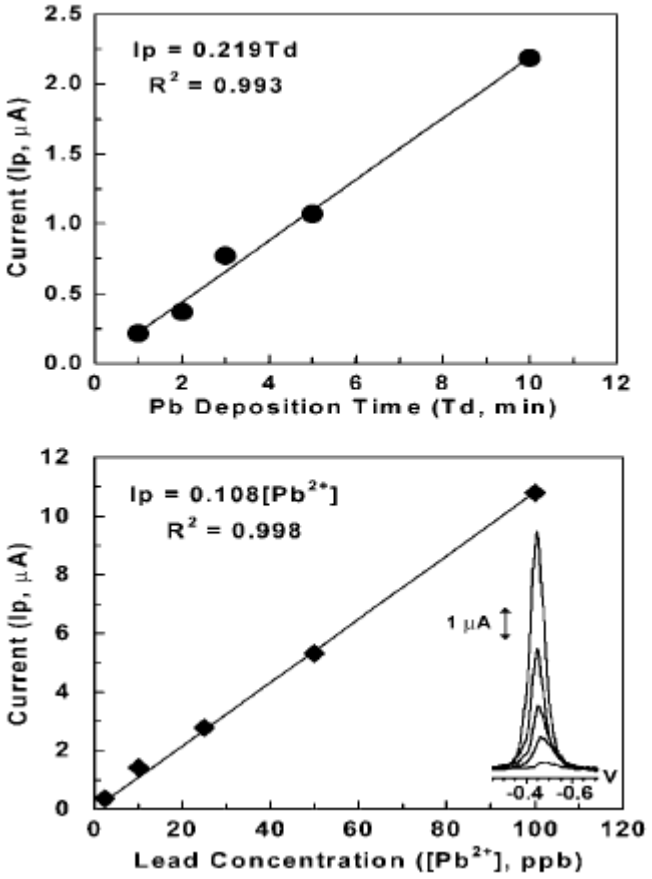


**Figure 14:** Optimization of current with Pb deposition time (top) and linear calibration between current and Pb2+ concentration (bottom).

Given these impressive results of sharp peaks, high sensitivity in the ppb range and low background noise, NT-containing electrodes have proven to be exceptionally effective in catalyzing electrochemical activity and minimizing common problems such as interference. These materials allow rapid, easy, precise, and repeatable measurements of trace concentrations of analytes that was not possible before.

## 2.3 FIELD EFFECT TRANSISTORS BASED ON CARBON NANOTUBES

Field effect transistors (FETs), consisting of metal oxides and silicon have been used for decades for everyday electronic applications; thousands of these devices are fabricated on microchips that make up devices such as computers. FETs have the general set up of a layer of silicon (Si), and on top of this is a layer of $SiO_2$. On either side of this composite are two electrodes known as the source and the drain, with a semiconducting material present carrying current between these electrodes. Applying a voltage to the gate electrode results switches the current-carrying material between conducting and insulating state. Many scientists have been designing FETs with an individual nanotube or a network of nanotubes situated between the source and drain electrode to carry the current.[72] Nanotubes are ideal for this application as they possess metallic and semiconducting properties, mentioned earlier. It is important to note that the current conducted by the metallic variety of nanotubes show no dependence on gate voltage, thus, they are not as useful for switching applications, thus semiconducting nanotubes are preferred for this purpose. A network of nanotubes may be added to such a device either by fabrication steps of mask-alignment, photoresist application and lift-off, or by simply dropcasting a nanotube dispersion between the two metallic electrodes on the silicon wafer. However, as a random network of nanotubes consist of ⅓ metallic nanotubes, these will contribute to the nanotube density reaching the percolation threshold necessary to carry current discussed earlier. Conductance of this network is easily modulated by changing the gate voltage, and the current vs. voltage behavior gives an indication of the charge transport mechanism of the FET. It has been shown consistently[73,74,75] that nanotube-based semiconducting FETs (NT-FETs) are characterized as *p*-type (because of atmospheric oxygen)[76], that is, are driven by

charge transport of holes. This was demonstrated by monitoring the increase of current as gate voltage was made more positive.

Since single-walled nanotube networks possess high carrier density and a surface-enhanced capacitance effect they make an ideal candidate for a sensing platform.[77] The conductance of the network has been shown to be sensitive to exposure of analyte molecules.[78] This behavior is attributed to the high surface-to-volume ratio and delocalized π electron density of the nanotubes. Conductance is affected by electron density being donated to or from the nanotube network by the analyte molecule. In the case of a *p*-type nanotube network, as it becomes more electron deficient (due to exposure of an electron-withdrawing molecule), the conductance should increase, as more holes are being injected and the majority charge carrier is more abundant. Conductance should predictably decrease as an electron-donating molecule injects negative charge density into the *p*-type network, and holes are withdrawn from the network, diminishing charge transport. These effects are reversed in the case of an *n*-type network which is formed by adding donor elements such as nitrogen atoms to the nanotube network. [79]

The sensitivity and selectivity of this NT-FET electrochemical sensor must be refined in order for it to be used as a practical device for environmental, medical and defense analysis. Many attempts have been made to endow these networks with the capability of better discrimination of chemical vapors and metal ions; these efforts have entailed the use of peptide sequences[80] and ion-exchanging polymers[80], among others.

The first model, using peptide sequences to detect $Ni^{2+}$ and $Cu^{2+}$, involves exposing an FET that already contains a SWNT network to a solution containing peptide-modified pyrrole or aniline (Ani) in an electrochemical cell.[80] After applying a potential to the SWNT network,

pyrrole (Py) or aniline (Ani) monomers are polymerized and deposited onto the network. The polymer and SWNTs have numerous noncovalent interactions which maintain the integrity of the nanotube network while making it selective to heavy metal ions using peptides of different sequences. A sensor array may be composed of a chip containing many SWNT-FETs that are each functionalized with varying peptide sequences which have selectivity for different analyte species. SWNT-FETs modified with Py-$His_6$ experienced a positive shift in the drain current versus gate voltage curves due to π-π stacking[81,82] between the polymers and SWNTs. These interactions become stronger as they accumulate. The modification of the SWNT surface was verified by AFM images showing a change in morphology after addition of the polymer and peptide sequence. Py-$His_6$ was used because of the high adsorption of histidine residues on the walls of carbon nanotubes, and $Ni^{2+}$ is known to chelate with histidine. [83] Gly-Gly-His (GGH) was added to polyaniline- and polypyrrole-SWNTs for $Cu^{2+}$ detection.[84]

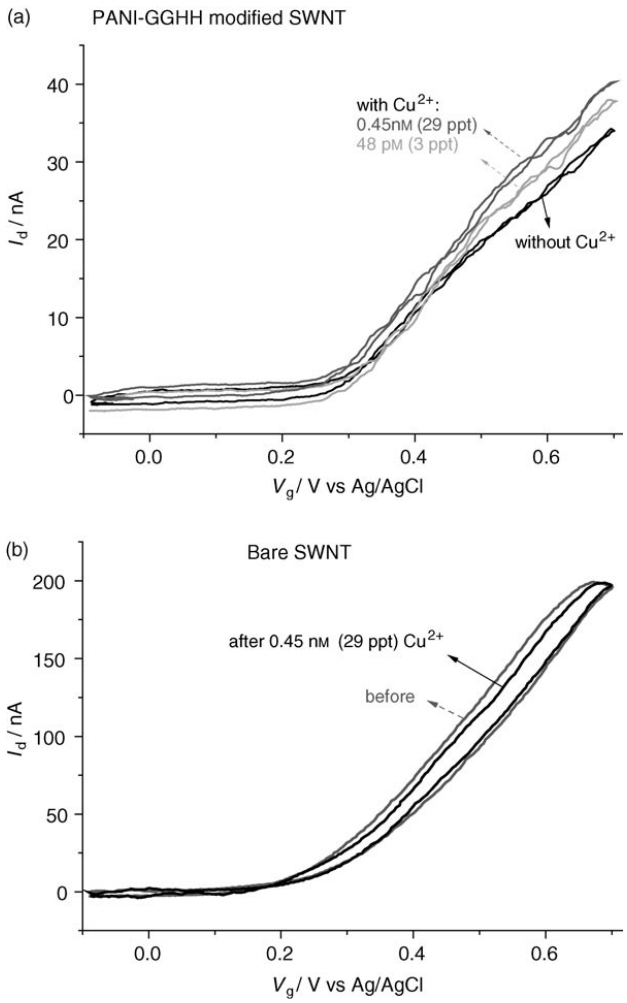


**Figure 15:** Decrease in gate voltage as a function of increase in the log of [$Ni^{2+}$] in nM (Top) Increase in conductance response as function of increase in log of [$Ni^{2+}$] in nM (Bottom). Adapted from Reference 79.

After the peptide-conjugated polymer was electrodeposited on the SWNT-FET, heavy metal ions were injected into the sample cell. Trapping of the metal ions by chelation with the

peptides results in decreased interaction between the peptide and the SWNT-FET. This is reflected in a change in conductance of the network as $Ni^{2+}$ is added. The FET exhibits *n*-type behavior when $Ni^{2+}$ is added, that is, conductance increases as potential ($V_g$) is made more negative. When $Ni^{2+}$ was added to bare SWNT-FET, the electronic behavior remains *p*-type; indicating that selective chelation of $Ni^{2+}$ with the peptide is responsible for the conversion of the SWNT-FET to *n*-type. The important analytical implication of this is the determination of $Ni^{2+}$ concentration as a function of negative potential shift, as $V_g$ was shown to be linearly related to the log [$Ni^{2+}$], with a detection limit in the $10^{-12}$ M range. The effect of [$Ni^{2+}$] on the Py-$His_6$-SWNT-FET is reversible: the chelated metal ions may be dissociated upon the addition of acid, which recovers the device current.

The PANI-GGH-SWNT-FET showed sensitivity to $Cu^{2+}$, and the devices yielded a negative shift in conductance upon $Cu^{2+}$ exposure. The effect of $Cu^{2+}$ on the polymer-peptide and the electronic behavior of the SWNT-FET is similar to that of $Ni^{2+}$ on Py-$His_6$-SWNT-FET. The SWNT-FET becomes *n*-type as the polymer-peptide has greater affinity for the chelated metal ions than for the SWNT network. The sensitivity of this system may be improved by adding another His residue to the peptide for increased chelation. Conductance was linearly related to $Cu^{2+}$ concentration. The limit of $Cu^{2+}$ detection was found to be in the $10^{-12}$ M range. This system offers superior sensitivity and selectivity as the peptide sequences are designed to have optimal chelation for the metal ion. The FET setup enables rapid, repeatable and reversible results. The system may be tuned to detect other metal ions by customizing the peptide sequence, and electron behavior may be optimized by choice of polymer.[79]

# 3.0 NONCOVALENT FUNCTIONALIZATION OF NANOTUBES WITH CHELATING LIGANDS FOR METAL ION DETECTION

Detection of metal ions for physiological and environmental monitoring has been carried out by water-soluble chelating ligands that are specifically designed to coordinate a metal ion and result in a color change of the solution upon metal-ligand complexation. Molecules used for this purpose are generally aromatic with a highly conjugated π electron system and are Lewis bases. Ferrozine[85,86] (IUPAC name: 3-(2-pyridyl)-5,6-diphenyl-1,2,4-triazine-4',4''-disulfonic acid sodium salt) complexes with $Fe^{2+}$ in a 3:1 stoichiometry; and neocuproine[87] (IUPAC name: 2,9-dimethyl-1,10-phenanthroline) which complexes with $Cu^{+}$ in a 2:1 stoichiometry. These chelating ligands were obtained from Sigma-Aldrich (St. Louis, MO). The structures of these complexes are given below:

a)

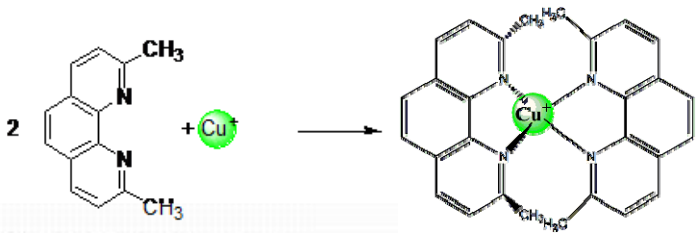


b)

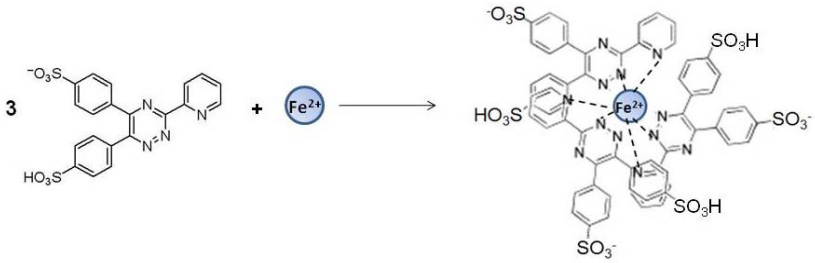


**Figure 16:** a) Chelation of two neocuproine ligands with one $Cu^{+}$ ion to form a tetrahedral complex. b) Chelation of three ferrozine ligands with one $Fe^{2+}$ ion to form octahedral complex.

Radiation absorption is caused by the excitation of electrons from an atom or molecular orbital with high electron density to an atom or molecular orbital with lower electron density. Interaction of the chelating ligand with the metal ion results in a color change and a strong absorption band upon complexation due to charge transfer between the ligand and the metal ion.[88] If the metal is in a higher oxidation state, absorption bands may be due to charge transfer from the σ or π electrons of the ligand to the metal ion or, if the metal ion is in a lower oxidation state, such as $Fe^{2+}$, an electron in the nonbonding *d* orbital of the metal ion transitions to a nonbonding orbital of the ligand, and the π system of the ligand is capable of back donation, resulting in an absorption band in the visible region.[86] For Ferrozine-$Fe^{2+}$complex dissolved in DI water, a purple-magenta colored solution is formed with $\lambda_{max}$=524 nm.[84] When $Cu^{+}$ successfully complexes with two neocuproine molecules in DI water, a blue solution is formed with a $\lambda_{max}$ at 450 nm. [85]

a)  b) 

**Figure 17:** a) Ferrozine-$Fe^{2+}$ complex in DI water. b) Neocuproine-$Cu^{+}$ complex in DI water.

Since absorbance is related to concentration, a standard curve of absorbances of known concentrations is used to identify the concentration of $Fe^{2+}$ in an unknown sample to which ferrozine has been added. This analytical strategy, using neocuproine, is used to quantify $Cu^{+}$. Since this method is based on UV-Vis spectroscopy and color observation, it is time consuming, expensive and not portable. We hypothesized that the sensing mechanism is based on the change in resistance of the nanotube network as a result of the metal-ligand complexation reaction and this change in resistance occurs as a function of metal ion concentration we wish to quantify. A potential outcome of this research is the development of a more economical and precise electrochemical sensor that can be used on-site.

Series of varying concentrations of the pre-formed complexes of ferrozine and $Fe^{2+}$ and neocuproine and $Cu^{+}$ were prepared. For the case of $Fe^{2+}$, iron (II) chloride was dissolved in DI water with excess ascorbic acid (Sigma-Aldrich, St. Louis, MO) added to prevent oxidation of $Fe^{2+}$ to $Fe^{3+}$. Copper (I) chloride was simply added to DI water. 1:100 (10 µL of 0.1 M solution in 1 mL DI water) serial dilution of a stock solution of pre-formed complex gave test solutions in a range of $10^{-13}$ M to 0.1 M.

Thin films of arc-discharge SWNTs (Carbon Solutions, Inc., Riverside, CA) were formed by spray-coating quartz plates with SWNT-DMF dispersion. DMF (dimethylformamide) was obtained from Sigma-Aldrich and was used without further purification. UV-Vis-NIR spectra were obtained on a Perkin-Elmer Lambda 900 Spectrometer.

Analysis of the UV-Vis-NIR spectra peaks are used to monitor the interaction of the chelating ligand (ferrozine, neocuproine) with the SWNT thin film and to verify occurrence of the ligand complexation with $Fe^{2+}$ or $Cu^{+}$. The heights of the $S_{11}$ and $S_{22}$ bands are used to follow the transfer of electron density between the analyte molecule and valence band of the SWNT. The decrease of the $S_{11}/S_{22}$ absorbance ratio illustrates electron density going from the SWNT network to the LUMO of the analyte, while increase of this ratio indicates electron density going from the HOMO of the analyte to the valance band of the SWNT. The addition of $Cu^{+}$ to neocuproine-SWNT shows a pronounced decrease in the absorbance of the $S_{11}$ transition, which suggests the SWNT network is losing electron density to the neocuproine-$Cu^{+}$ complex. This decrease is not as obvious for the Ferrozine-$Fe^{2+}$ case, so the

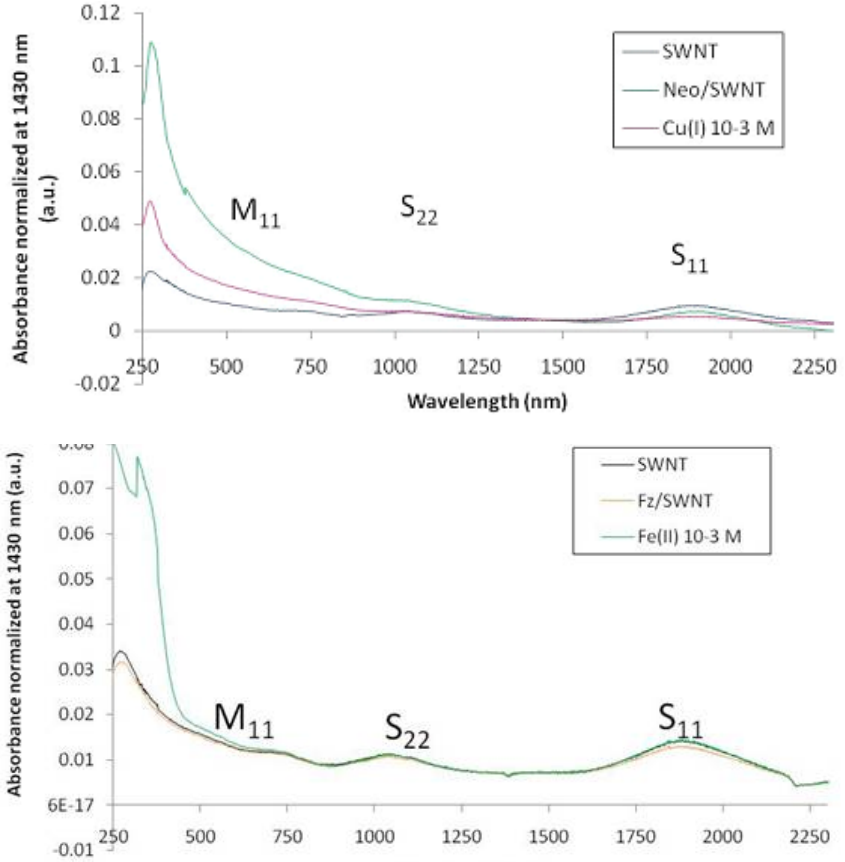


**Figure 18:** Ferrozine-$Fe^{2+}$ applied to SWNT thin film (top) Neocuproine-$Cu^{+}$ applied to SWNT thin film (bottom).

electron transfer behavior cannot be concluded from this experiment.

This information from the UV-Vis-NIR spectra should help predict the change in conductance of the *p*-type SWNT electronic device upon the addition of these complexed metal ions. If the *p*-type SWNT network (condutance driven by holes) transport of holes) is losing electron density to the neocuproine-$Cu^{+}$ complex, as suggested in the spectra, then an increase in the conductance of the SWNT device should be expected upon increased exposure to this complex.

The device containing SWNTs is used for measuring change in conductance upon exposure to metal ions in aqueous solution and complexed the appropriate ligand and the results are given below: This device was connected to a Keithley 2400 sourcemeter which served as power supply and provided a constance voltage for conductance measurements.

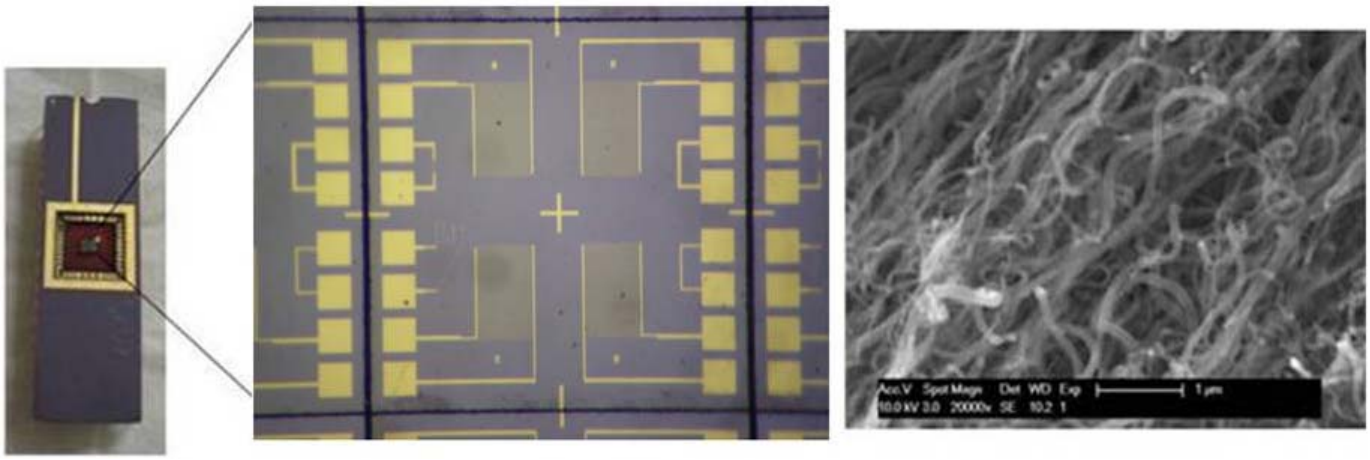

**Figure 19:** Optical photograph of CERDIP package (left) containing a silicon chip with four interdigitated Au electrodes (middle). Scanning electron microscopy (SEM) image of SWNT network deposited on the chip (right). Images obtained by the Star Lab.

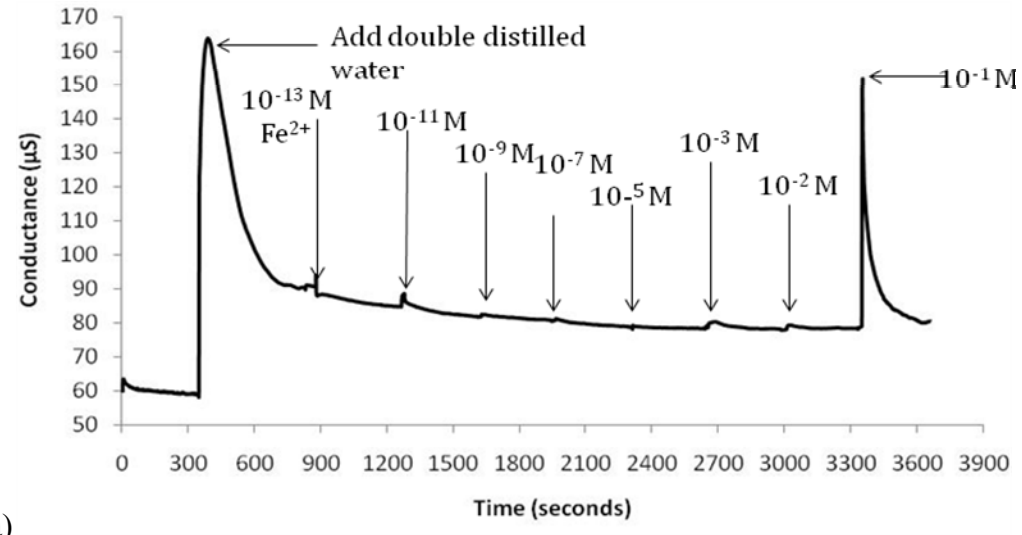
Add double distilled water
$10^{-13}$ M $Fe^{2+}$
$10^{-11}$ M
$10^{-9}$ M
$10^{-7}$ M
$10^{-5}$ M
$10^{-3}$ M
$10^{-2}$ M
$10^{-1}$ M
Conductance (µS)
Time (seconds)

a)

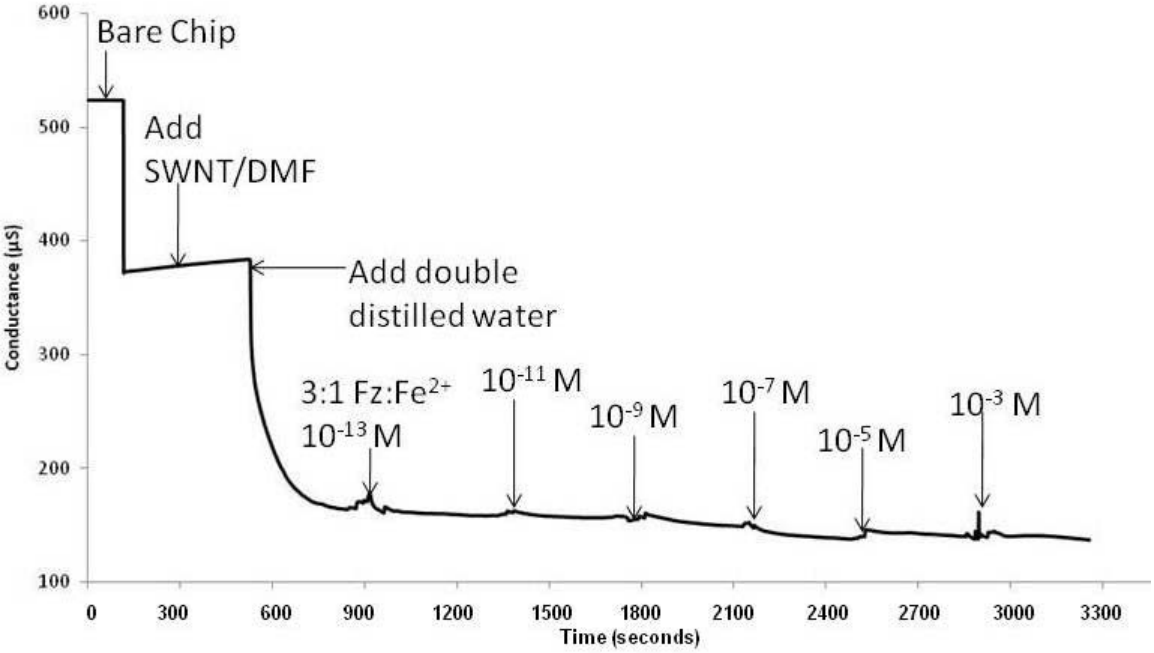
Bare Chip
Add SWNT/DMF
Add double distilled water
3:1 Fz:$Fe^{2+}$ $10^{-13}$ M
$10^{-11}$ M
$10^{-9}$ M
$10^{-7}$ M
$10^{-5}$ M
$10^{-3}$ M
Conductance (µS)
Time (seconds)

b)

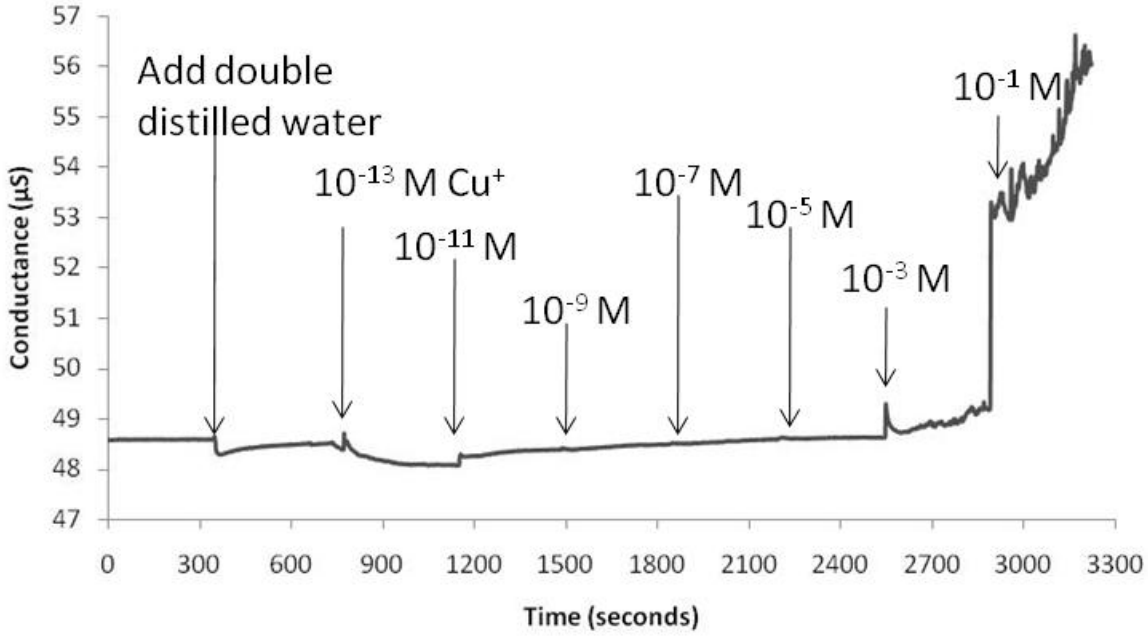


c)

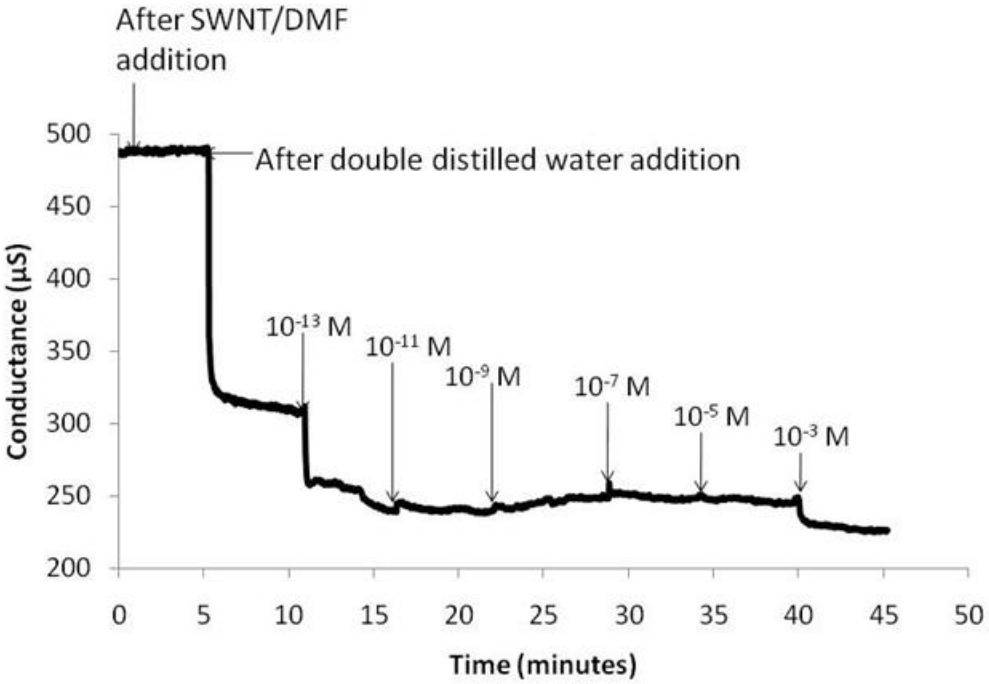


d)

**Figure 20**: a) $Fe^{2+}$ added to bare SWNT, b) 3:1 ferrozine:$Fe^{2+}$ complexes added, c) $Cu^{+}$ added d) 2:1 Neoucproine:$Cu^{+}$ added.

The devices containing chelating ligands did not show markedly improved sensitivity toward metal ions than bare SWNTs. This suggests that the electron transfer between the metal ion, ligand and SWNT was not transduced to a practical analytical signal.

The addition of double distilled water to the chemiresistors gave conflicting results when monitoring metal ion effect on conductance. The purpose of adding double distilled water was to provide a constant hydration layer on the nanotube network that would respond only to the metal ion added, and not be affected by the mere prescence of a drop of solution. It is perplexing to observe an increase in conductance upon addition of DI water to the device in some cases, and a decrease in conductance in others. Possible explanations for this behavior include variability in the thickness of the SWNT thin film used for the electrochemical measurements. As evidenced from the conductance data, it was difficult to achieve reproducible and similar conductance values for the bare nanotube networks for each experiment.

The adverse effects of adding drops of solution to the device for conductance measurements, including noise, may be avoided by using a flow injection system.[89] This allows for the level of solution above the network to remain constant, minimizing errors in conductance measurements due to changes in volume, thus accurately monitoring metal ion effect on conductance, giving a better picture of charge transport, sensitivity and selectivity, parameters important to sensor development.

Ensuring that the system is studying only the components of interest, that is, effect of nanotube network conductance is consistently demonstrated to be sensitive to the type and concentration of the metal ion, and not prone to results that vary despite employing identical synthesis and analytical methods for every trial, is paramount to obtaining significant

information elucidating the mechanism of nanotube network conductance modulation, and apply it to rational design of useful sensors.

The technique of using conjugated molecules to chelate metal ions and form complexes that are UV-Vis-NIR active to quantify and identify ions has been a convenient and effective strategy for nearly a century. The advantages of this system have been ease and versatility of ligands and metal-ion selectivity. However, the analysis is not rapid, requires bulky equipment, prone to interference affecting precision and accuracy of measurement of desired ion and has inadequate detection limits. Since charge transfer is the basis for the complexation reaction observed in UV-Vis-NIR, conductance measurements should be a viable means of metal ion detection. Carbon nanotube networks are being investigated as a platform for sensitive and rapid study of conductance behavior influenced by metal ions. Since carbon nanotubes do not have inherent selectivity for metal ions, chemical treatment, functionalization and addition of chelating ligands must be explored. Understanding the interaction of between carbon nanotubes and ferrozine or neocuproine will enable the production of portable electrochemical sensors for iron and copper ions with detection limits and analysis times rivaling current devices and spectroscopic methods.

## BIBLIOGRAPHY


[1] Bontidean, I.; Ahlqvist, J.; Mulchandani, A., et al. *Biosensors and Bioelectronics*. **2003**, *18*, 547-553

[2] Shaw, M., Haddad, P. *Environment International*, **2004**, *30*, 403-431

[3] Zaporozhets, O.; Petruniock, N.; Bessarabora, O.; Sakhan, V. *Talanta,* **1999**, *49*, 899-906

[4] Chumbimuni-Torres, K.; Calvo-Marzal, P; Wang, J.; Bakker, E. *Anal. Chem*. **2008**, *80*, 6114-6118

[5] Tanaka, N.; Kobagashi, H.; Ishizuka, N. *J. Chromatography A*, **2002**, *965*, 35-49

[6] Abe-Onishi, Y.; Sugimoto, N.; Tanamoto, K. *J. Chromatography A.* **2004**, *1040*, 209-214

[7] Larsen, E.; Hansen, M.; Fan, T.; Vahl, M. *J. Anal. Atom. Spectrom*., **2001**, *16*, 1403-1408

[8] Hu, Yang, Yin, Yao. *Talanta*, **2002**, *57*, 751-6

[9] Li, Z.; Yang, G.; Wang, B.; Jiang, C.; Yin, J. *J. Chromatography A*, **2002**, *971*, 243-283

[10] Hu, Q.; Yang, Q.; Zhao, Y.; Yin, J. *Anal Bioanalchem*, **2003**, *375*, 831-5

[11] Paull, B., Haddad, P.R. *Trends in Anal. Chem*. **1999**, *18*, 107-114

[12] Yordanov, A.T., Roundhill, D.M. *Coord. Chem. Rev*. **1998**, *170*, 93-124

[13] Petrat, F.; Weishat, D.; Lensen, M.; de Groot, H.; Sustmann, R.; Rauen, U. *Biochem. J.* **2002**, *362*, 137-147

[14] Chan, W.H.; Yang, R.H.; Wang, K.M. *Analytica Chimica Acta*, **2001**, *444*, 261-269

[15] Winkler, J.; Bower, C.; Michelet, V. *J. Am. Chem. Soc*. **1998**, *120*, 3237-3242

[16] Sumner, J.; Westerberg, N.; Stoddard, A.; Fierke, C.; Kopelman, R. *Sens. Act. B.* **113**, *2006*, 760-767

[17] Saari, L.A., Seitz, W.R. *Anal. Chem*., **1983**, *55*, 667-670

[18] Al-Kindy, S.M.Z., Suliman, F.O., Salama, S.B. *Microchemical Journal,* **2003**, *74*, 173-179

[19] Kalvoda, R., Kopanica, M. *Pure & Appl. Chem*., **1989**, *61*, 97-112

[20] Kounaves, S.P. "Voltammetry Techniques" *Chapter 37 Handbook of Instrumental Techniques for Analytical Chemistry* Prentice Hall, **1997,** p.720-722.

[21] Yong, L., Armstrong, K.C., Dansby-Sparks, R.N., Carrington, N.A., Chambers, J.Q., Xue, Z. *Anal. Chem*., **2006**, *78,* 7582-7587.

[22] Wang, J., Lu, J. *Electrochem. Comm*. **2002**, *2*, 390-393.

[23] Bausells, J., Carrabina, J., Errachid, A., Merlos, A. *Sens. and Act. B,* **1999**, *57*, 56-62

[24] Bartic, C., Campitelli, A., Borghs, S. *Appl. Phys. Lett*. **2003**, *82*, 475-477.

[25] Bergveld, P. *Sens and Act. B.* **2003**, *88*, 1-20

[26]Schon, J.; Bao, Z. *Appl. Phys. Lett.* **2002**, *80*, 332-333

[27] Janata, J.; Joscowicz, M. *Nat. Mater*. **2003**, *2*, 19-24.

[28]Gerard, M.; Chaubey, A.; Malhotra, B. *Biosens. and Bioelect*. **2002**, *17*, 345-359.

[29]Star, A.; Han, T.; Grüner, G. *Nano. Lett*. **2003**, *3*, 1421-1423

[30]Javey, A.; Guo, J.; Dai. H. *Nature*, **2003**, *424*, 654-657.

[31] Kim, W.; Javey, A.; Dai, H. *Nano Lett*, **2003**, *3*, 193-198

[32] Taillades, G.; Valls, O.; Bratov, A.; Dominguez, C.; Pradel, A.; Ribes, M. *Sens. Act. B* **1999**, *59*, 123-127

[33] Rahman, M.; Park, D.; Won, M.; Park, S.; Shim, Y. *Electroanalysis* **2004**, *16*, 1366-1370

[34] Errachid, A.; Zine, N.; Samitier, J.; Bausells, J. *Electroanalysis* **2004**, *16*, 1843-1851

[35] Divjak, B.; Franko, M.; Novič, M. *J. Chromatography A.* **1998**, *829,* 167-174

[36] Bashir, W.; Paull, B. *J. Chromatography A.* **2002**, *942*, 73-82

[37] McMurry, John. *Organic Chemistry*, Sixth edition, Brooks/Cole, Thomson Learning, 2004, p.7

[38] Iijima, S. *Nature*, **1991**, *354*, 56-58

[39] Iijima, S.; Ichihashi, T. *Nature*, **1993**, *363*, 603-605

[40] Bethune, D.S.; Klang, C.H.; De Vries, M.S., Gorman, G.; Savoy, R.; Vazquez, J.; Beyer, R. *Nature* **1993**, *363*, 605-607.

[41] Odom, T.; Huang, J.; Lieber, C. *Nature* **1998**, *391*, 62-64

[42] Dumitrescu, I.; Wilson, N.; Macpherson, J. *J. Phys. Chem. C.* **2007**, *111*, 12944-12953

[43]Wilson, N.; Guille, M.; Macpherson, J. *Anal. Chem*. **2006**, *78*, 7006-7015

[44] Snow, E.; Novak, J.; Campbell, P. *J. Vac. Sci. Technol., B.* **2004**, *22*, 1990-1994

[45] Wildöer, J.; Venema, L.; Dekker, C. *Nature*, **1998**, *391*, 59-62

[46] Heller, I.; Kong, J.; Lemay, S. *J. Am. Chem. Soc.* **2006**, *128*, 7353-7359

[47] Ryabenko, A.; Dorofeeva, T.; Zvereva, G. *Carbon*, **2004**, *42*, 1523-1535

[48] Kauffman, D.; Star, A. *Small* **2007**, *3*, 1324-1329

[49] Hu, H.; Bhowmick, P.; Haddon, R. *Chem. Phys. Lett*. **2001**, *345*, 25-28

[50] Hamon, M.; Hu, H.; Haddon, R. *Chem. Phys. Lett*. **2001**, *347*, 8-12

[51] Mawhinney, D.; Naumenko, V.; Smalley, R. *Chem. Phys. Lett*. **2000**, *324*, 213-216

[52] Kuznetsova, A.; Popova, I.; Smalley, R. *J. Am. Chem. Soc.* **2001**, *123*, 10699-10704

[53] Felten, A.; Bittencourt, C.; Charlier, J. *J. Appl. Phys*., **2005**, *98*, 0743081-0743089

[54] Gao, H.; Kong, Y.; Ozkan, C. *Nano Lett.* **2003**, *3*, 471-473

[55] Pantarotto, D.; Partidos, C.; Bianco, A. *J. Am. Chem. Soc*., **2003**, *125*, 6160-6164

[56] Zorbas, V.; Ortiz-Acevedo, A.; Musselman, I. *J. Am. Chem. Soc.* **2004**, *126*, 7222-7227

[57] Hrapovic, S.; Liu, Y.; Luong, J. *Anal. Chem*. **2004**, *76*, 1083-1088

[58] Farmer, D.; Gordon, R. *Nano Lett.* **2006**, *6*, 699-703

[59] Qu, L.; Martin, R.; Allard, L. *J. Chem. Phys.* **2002**, *117*, 8089-8094

[60] Chen, R.; Zhang, Y.; Dai, H. J. *Am. Chem. Soc*. **2001**, *123*, 3838-3839

[61] Jin, H.; Heller, D.; Strano, M. *Nano Lett*. **2008**, *8*, 4299-4304

[62] Brege, J; Gallaway, C.; Barron, A. *J. Phys. Chem. C*. **2009**, *113*, 4270-4276.

[63] Moore, V.; Strano, M.; Smalley, R. *Nano Lett*. **2003**, *3*, 1379-1382.

[64] Bachilo, S.; Strano, M.; Wiseman, R. *Science* **2002**, *298*, 2361-2366.

[65] Wang, Z.; Liu, J.; Luo, G. *Analyst.* **2002**, *127*, 653-658

[66] Luo, H.; Shi, Z.; Zhuang, Q. *Anal. Chem*. **2001**, *73*, 915-920

[67] Campbell, J.; Sun, L.; Crooks, R. *J. Am. Chem. Soc.* **1999**, *121*, 3779-3780

[68] Ferdnández-Abedul, M.; Costa-García, A. *Anal Bioanal Chem* **2008**, *390*, 293-298

[69] Gao, Z.; Wei, W.; Guo, M. *Electroanalysis*, **2006**, *18*, 485-492

[70] Tu, Y.; Lin, Y.; Ren, Z. *Electroanalysis*, **2005**, *17*, 79-84

[71] Yi, H. *Anal Bioanal Chem*, **2003**, *377*, 770-774.

[72] Tans, S.; Verschueren, A.; Dekker, C. *Nature,* **1998**, *393*, 49-52

[73] Martel, R.; Schmidt, T.; Avouris, Ph. *Appl. Phys. Lett*. **1998**, *73*, 2447-2449

[74] Derycke, V.; Martel, R.; Avouris, Ph. *Appl. Phys. Lett*. **2002**, *80*, 2773-2775

[75] Liu, K.; Burghard, M.; Bernier, P. *Appl. Phys. Lett*. **1999**, *75*, 2494-2496

[76] Bradley, K.; Cumings, J.; Grüner, G. *Nano Lett.* **2003**, *3*, 639-641

[77] Forzani, E.; Li, X.; Nagahara, L. *Small,* **2006**, *2*, 1283-1291

[78] Kong, J.; Franklin, N.; Dai, H. *Science*, **2000**, *287*, 622-625

[79] Xiao, K.; Liu, Y.; Xhu, D. *J. Am. Chem. Soc.* **2005**, *127*, 8614-8617

[80] Star, A.; Han, T.; Stetter, J. *Electroanalysis,* **2004**, *16*, 108-112

[81] Latil, S.; Roche, S.; Charlier, J. *Nano Lett.* **2005**, *5*, 2216-2219

[82] Tournus, F.; Latil, S.; Charlier, J. *Phys. Rev. B.* **2005**, *72*, 0754311-0754315

[83] Hu, P.; Loo, J.; *J. Am. Chem. Soc.* **1995**, *117*, 11314-11319

[84] Forzani, E.; Zhang, H.; Tao, N. *Environ. Sci. Technol*. **2005**, *39*, 1257-1262

[85] Faulkner, S.; Hintz, P.; Ashby, S. (1999). "Evaluation of Colorimetric Methods for Measuring Reduced (Ferrous) Iron," *Water Quality Technical Notes Collection* (WQTNPD-02), U.S.

Army Engineer Research and Development Center, Vicksburg, MS. www.wes.army.mil/el/elpubs/wqtncont.html

[86] Harris. D. *Quantitative Chemical Analysis*, Sixth edition W.H. Freeman 2003.

[87] Gahler, A. *Anal. Chem*. **1954**, *26*, 577-579.

[88] Némcová, I.; Čermáková, L.; Gasparič, K. *Spectrophotometric Reactions*, Marcel Dekker, New York, 1996, 7-8.

[89] Covington, J.; Gardner, J.; Briand, D.; de Rooij, N. *Sens. Act. B.* **2001**, *77*, 155-162